Multiple ground state competition under pressure in β-$Sr_{0.33}V_2O_5$

Touru Yamauchi,* Hiroaki Ueda, Jun-Ichi Yamaura, and Yutaka Ueda
Material Design and Characterization Laboratory, Institute for Solid State Physics, University of Tokyo, 5-1-5 Kashiwanoha, Kashiwa, Chiba, 277-8581, Japan

(Received 26 November 2006; revised manuscript received 30 November 2006; published 29 January 2007)

Magnetic susceptibility and resistivity of β-$Sr_{0.33}V_2O_5$ were precisely measured under pressure. With increasing pressure, the charge order transition is suppressed and furthermore anomalous behaviors are observed, indicating two or more phases in the charge ordered phase and two phases in the charge disordered phase. High-pressure x-ray oscillation photographs confirm different modulation vectors in these phases, which suggests the "devil's staircase"-type phase transition as observed in α'-NaV_2O_5. The obtained P-T phase diagram displays competition among multiple ground states under pressure.

DOI: 10.1103/PhysRevB.75.014437 PACS number(s): 71.30.+h, 74.62.Fj

Competition among several ground states is a central issue in condensed matter physics, since fascinating phenomena in highly correlated electron system such as high-T_c superconductivity and colossal magnetoresistance appear with such competition.[1] A series of quasi-one-dimensional (q1D) vanadium oxide conductors, β-vanadium bronzes, represented as a chemical formula β-$A_{0.33}V_2O_5$ (A=Li, Na, Ag, Ca, Sr, and Pb), give us a good stage to study such competitions. Among them, β-$Na_{0.33}V_2O_5$ has been an epoch-making compound because of the first superconductor among vanadium oxides, where a pressure-induced *superconducting* (SC) phase competes with a *charge ordering* (CO) phase in a peculiar pressure-temperature (P-T) electronic phase diagram.[2,3]

The monoclinic crystal structure of β-$A_{0.33}V_2O_5$ consists of a characteristic V_2O_5 framework and A cations as illustrated in Fig. 1. The V_2O_5 framework is formed by $(V1)O_6$, $(V2)O_6$ octahedra and $(V3)O_5$ pyramids, where V1, V2, and V3 are three distinct V sites. Each polyhedra forms infinite chains along the b axis (the q1D conduction axis). The A cations which are represented as small white balls are located in the straight tunnels along the b axis and occupy only one

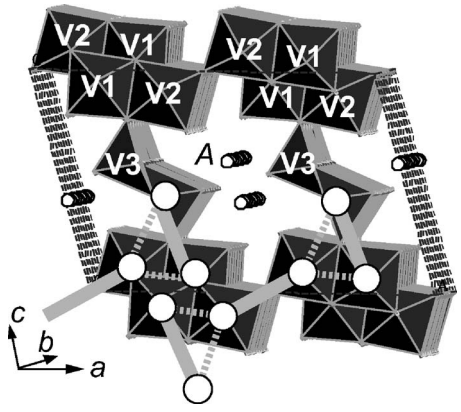

FIG. 1. The crystal structure of β-$A_{0.33}V_2O_5$ projecting along the b axis. A ions (small white balls) and VO_6/VO_5 polyhedra are illustrated with site assignments V1, V2, and V3. The six large white balls and the connecting gray boldfaced solid-thin broken lines represent an electronic model which will be called "coupled 2-leg ladders."

of the two nearest-neighboring A sites in the same a-c plane. The crystal structure has a space group of $C2/m$ in random occupancy of A cation at the array of A sites. In contrast, alternatively ordered A cation in the A sites results in a space group $P2_1/a$ with a twice unit cell along the b axis. This A cation order-disorder transition is observed at 230 K in β-$Na_{0.33}V_2O_5$, while in β-$Sr_{0.33}V_2O_5$, A cations order even at room temperature.[4] For commonality, in the following part we will consider the monoclinic $C2/m$ structure without doubling the unit cell along the b axis as the fundamental structure for a series of β-vanadium bronzes.

In this figure, we also illustrate schematically the electronic model for β-$Sr_{0.33}V_2O_5$ proposed by the recent Hückel tight-binding calculation.[5] This calculation revealed that the electronic structure can be considered as weakly coupled two kinds of two-leg ladders; V1-V3 and V2-V2. Both two ladder running along the b axis are exhibited by white large balls (V atoms) and gray boldfaced solid lines (namely, these lines represent rungs of the ladders). The coupling between these two ladders are also illustrated by gray thin broken lines. Note the quite small transfer integrals even between neighboring ladders which *are not* connected by the broken lines allow us to consider the system as coupled only three (two V1-V3 and one V2-V2) ladders as shown in Fig. 1. We will discuss the electromagnetic properties of this compound based on this model.

The CO transition is a common characteristic nature of β-vanadium bronzes except for A=Pb compound[6,7] and the CO results in a superstructure with a common sixfold periodicity along the b axis. The sixfold periodicity can be described as two fold by A-cation order multiplied by three fold by CO in β-$Na_{0.33}V_2O_5$.[4,8] The CO transitions are followed by antiferromagnetic transitions in A^+ compounds, while in A^{2+} compounds they are followed by spin-gap behaviors.[9] The spin gap nature was confirmed by NMR and inelastic neutron scattering on powder samples.[10,11]

In all A^+ compounds, the CO phases collapse under relatively high pressure ($\geq$7 GPa) and then SC phases appear.[12] On the other hand, divalent A^{2+} compounds β-$A_{0.33}V_2O_5$ (A=Ca, Sr, and Pb) do not show superconductivity, although the CO phases are suppressed under relatively low pressures (A=Ca/3.5 GPa, Sr/1.5 GPa).[13] Fortunately, β-$Sr_{0.33}V_2O_5$ has a very low critical pressure as expected from relatively

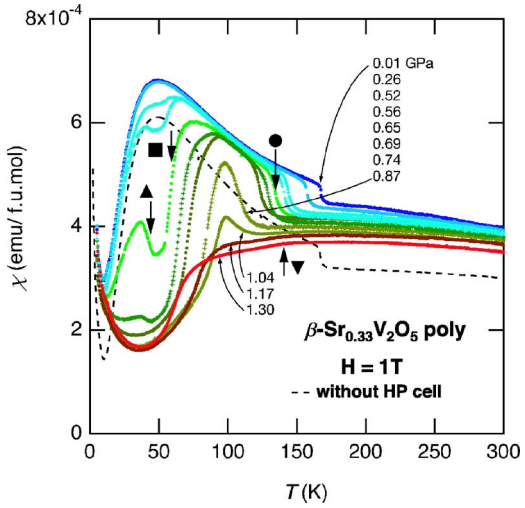

FIG. 2. (Color online) Temperature dependences of magnetic susceptibility of β-$Sr_{0.33}V_2O_5$ under several pressures. A curve drawn by a black broken line is obtained by an ordinal measurement without pressure cell. Eight bold curves with rainbow color (online) show the susceptibility under several pressures.

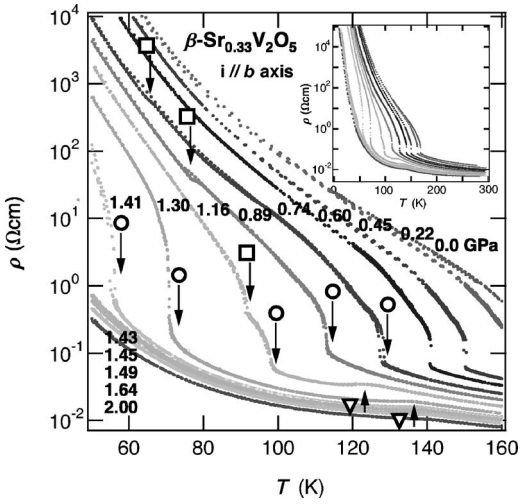

FIG. 3. Temperature dependences of resistivity under pressure. The inset shows overall view of ρ-T curves. The T_{CO} (open circles), T_d (open squares), and small kinks in a charge disorder phase, T_m (open inverted triangles) are clearly observed. On the other hand, neither T_d nor T_i were observed blow 0.8 GPa.

large volume change of crystal unit cell at T_{CO}.[4] Thus, this compound gives a good chance to observe how the CO phase collapses under pressure. We have carefully measured both magnetic susceptibility and resistivity under pressure. In this paper, we report anomalous behaviors associated with some unusual phase transitions, which indicates the competition of multiple ground states in this A^{2+} compound.

The magnetic susceptibility χ of polycrystalline samples (about 20 mg) under various pressures were measured in external field of 1 T by a commercial magnetometer MPMS-5s (Quantum Design Co. Ltd) equipped with a pressure cell made of a CuBe cylinder and ZrO_2 pistons. Daphne oil 7373 (Idemitsu Co. Ltd) was used as a pressure medium. In the measurements, the contribution from the pressure cell filled with Daphne oil and without sample was subtracted from the raw output signals of MPMS *in situ*. The resistivity of single crystal along the *b* axis (conductive direction) was measured by an ordinary four-probes method with several constant dc excitation currents, 0.1 μA, 10 μA, and 1 mA in a pressure cell made of NiCrAl hybrid CuBe cylinder and a WC piston with methanol-ethanol mixture (4:1) as a pressure medium. The x-ray oscillation photographs on a single crystal under high pressures were taken in a diamond-anvil cell with a refrigerator. We used a curved imaging plate and a monochromatic Mo-$K\alpha$ radiation x-ray source (rotating anode 21 kW, Mac Science Co. Ltd). The pressure medium was methanol-ethanol mixture (4:1). The typical exposure time was about 12 hours for one photograph.

The observed susceptibility versus temperature (χ-T) curves under various pressures are exhibited in Fig. 2. Two χ-T curves with and without the pressure cell at ambient pressure coincide well with each other except for paramagnetic offset which comes from the oversubtracted diamagnetic contribution of Daphne oil corresponding to the sample volume. By lowering temperature, the χ at ambient pressure shows a sudden increase at T_{CO}=168 K from Pauli paramagnetic behavior above T_{CO}, and then it shows low dimensional spin gap behavior with a broad maximum around 50 K. Unexpectedly, the χ-T curves show complex behaviors with the increasing pressure as shown in Fig. 2. With a slight increase of pressure up to 0.52 GPa, some hump appears around 50 K in addition to the jump at T_{CO}, and this hump grows as pressure further increases.

Some χ-T curves around 0.6 GPa clearly show three anomalies; the jump at $T_{CO}\sim$140 K (filled circle), anomalous drop at $T_d\sim$65 K (filled square) and sudden increase of χ at $T_i\sim$40 K (filled triangle). In other word, χ-T curves below T_{CO} anomalously drop between T_d and T_i. With further increasing pressure, both T_{CO} and T_i decrease, while T_d increases. The T_{CO} and T_d approach each other with increasing pressure and finally they merge above 1.1 GPa. On the other hand, the anomaly at T_i quickly becomes invisible and it was observed in the very narrow pressure region 0.5–0.7 GPa. In addition to these three anomalies, a kink marked with a filled inverted triangle was observed at $T_m\sim$140 K above 1.1 GPa. It should be noted that all observed χ-T curves show spin-gap behavior at lowest temperature. Very similar behaviors of χ-T curves under pressure have also been observed in the same A^{2+} compound, β-$Ca_{0.33}V_2O_5$.

Some transitions responsible for these anomalies in the χ-T curves were also observed in resistivity measurements as shown in Fig. 3. The inset shows an overall view of resistivity versus temperature (ρ-T) curves up to 2.0 GPa and the main panel shows macrograph of the inset. The CO transition (open circles) is clearly observed in these ρ-T curves and T_{CO} is also suppressed by elevating pressure. In addition, the second anomaly at T_d (open squares) is also observed as a kink in each ρ-T curve under 0.74–1.16 GPa, as shown in Fig. 3. On the other hand, the third anomaly at T_i observed in the χ-T curves was not observed presumably because of the significantly high resistivity at low temperature. The T_d increases with the increasing pressure and meets with T_{CO} above 1.2 GPa, agreeing with the results of the χ measure-

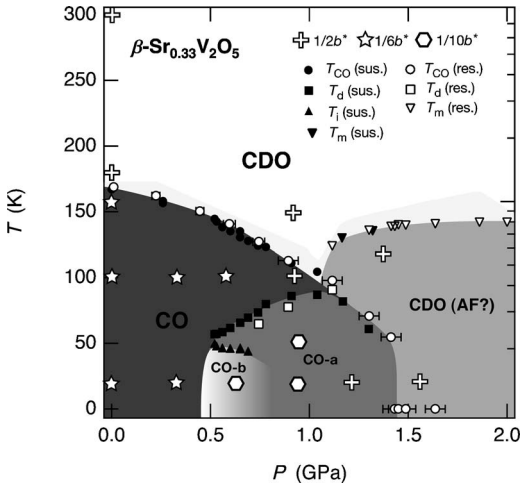

FIG. 4. Pressure-temperature (P-T) phase diagram of β-$Sr_{0.33}V_2O_5$. The filled and open symbols derived from susceptibility and resistivity measurements, respectively. Some x-ray oscillation photographs were taken at several points represented as a few kinds of symbols. The symbols exhibit observed superperiodicity along the b axis (see caption in Fig. 5).

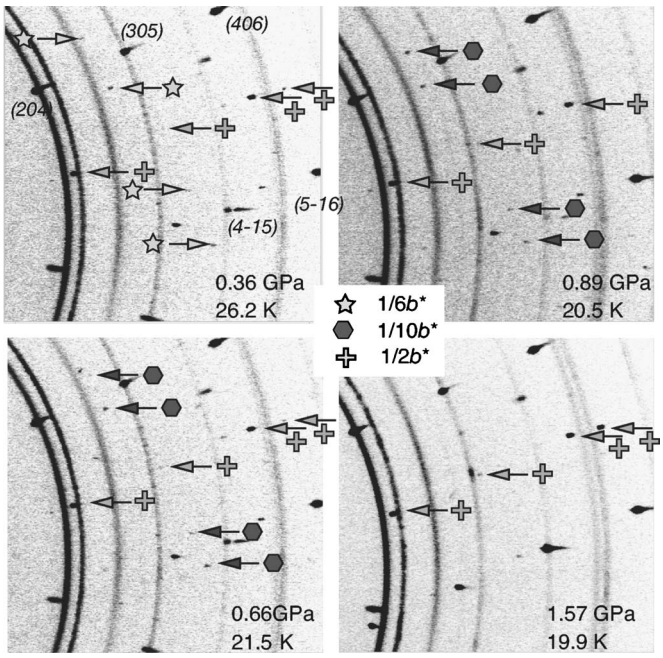

FIG. 5. Typical x-ray oscillation photographs taken under pressure at 20 K. Three kinds of superspots are observed with modulation vectors, $q=1/2b$, $1/6b$, and $1/10b$ which are exhibited by cross, star, and hexagon symbols, respectively.

ments. Furthermore an anomaly at T_m (open inverted triangles) was also observed above 1.2 GPa. With further increase of pressure up to about 1.5 GPa, the T_{CO} continuously decreases to the lowest temperature, while the T_m tends to increase at first and then saturates around 140 K. The insulating behaviors in the pressure-stabilized *charge disorder* phase (CDO) at low temperature region are explained in the lights of randomness driven strong localization which is probably caused by imperfections which arise from poor crystallinity. In q1D system, such imperfections should crucially affect the conduction nature of the crystals. Actually, recent doping studies on q1D organic conductors reveals randomness driven insulating behavior in spite of their q1D Fermi surfaces.[14]

Up to 7.5 GPa, the fourth anomaly at T_m remains and the system gradually becomes metallic without phase transition.[13] This means the insulating nature at lowest temperature is not caused by the transition at T_m. Here it should be emphasized that the ρ-T curve at 1.16 GPa clearly shows the three transitions at T_{CO}, T_d, and T_m. This means that T_d never penetrates into the CDO phase as T_m but merges into T_{CO} above 1.2 GPa, namely T_m is independent of T_d.

The P-T phase diagram constructed from the results of χ and ρ measurements is shown in Fig. 4. The transition temperatures of T_{CO}, T_d, T_i, and T_m are plotted in this phase diagram by several kinds of symbols mentioned above. These transition temperatures are defined as peak temperatures of $|\partial\chi/\partial T|$ and temperatures at distinct anomalies on ρ-T curves. The T_d's and T_{CO}'s from χ and ρ coincide well. At first, the P-T phase diagram is divided into the *charge ordering*/*charge disordering* phases by T_{CO}. In the CO phase, there exist at two or more phases as shown by the annotations, "CO," "CO-a," and "CO-b" in Fig. 4. The phase boundaries are drawn by T_{CO}, T_d, and T_i. The phase transitions at T_{CO}, T_d, and T_i should be closely related to the CO mechanism, while the transition at T_m is not the case. Although there is no direct evidence, we believe the transition at T_m is an antiferromagnetic (AF) ordering from the facts that many systems show a slight decrease of χ and ρ at AF transitions as observed in this study. Thus we can give one speculation for the absence of superconductivity in β-$Sr_{0.33}V_2O_5$; AF order is realized before the system falls into superconductivity. To verify AF order, much more microscopic study such as NMR or neutron scattering should be needed.

To elucidate what happens at these transitions, especially in CO phase, we have taken x-ray oscillation photographs of a single crystal at several temperature-pressure points represented by a few kinds of symbols (cross, star, and hexagon) in Fig. 4. Observed typical x-ray diffraction (XRD) patterns are shown in Fig. 5. In these patterns, three kinds of XRD superspots with $q=1/2b^*$, $1/6b^*$, and $1/10b^*$ are observed. The $q=1/2b^*$ is attributed to the Sr ordering, and the $q=1/6b^*$ and $1/10b^*$ result from CO. At ambient pressure, the $1/2b^*$ structure is observed in both CDO and CO regions and $1/6b^*$ superspots additionally appear at CO transition. At the lowest temperature, 20 K, the $1/6b^*$ structure remains up to 0.36 GPa and then $1/10b^*$ superspots appear instead of those of $1/6b^*$ superspots at 0.66 GPa. Under 0.90 GPa, $1/2b^*$ superspots (cross) keep their intensities and $1/10b^*$ superspots (hexagon) are also recognized below T_d. At 0.5 GPa (CO-b region), we have observed coexistence of $1/6b^*$ and $1/10b^*$ spots. From the shape of χ-T curves at this region (see the curve of 0.56 GPa in Fig. 2, it looks to drop at T_d and to return at T_i to the original curve) and the coexistence of two kinds of superspots, reentrant nature of the phase boundary between $1/6b^*$ and $1/10b^*$ phases is naturally conceivable. Above 1.2 GPa, the satellite peaks with $q=1/10b^*$ disappear and there exists no observable superspot

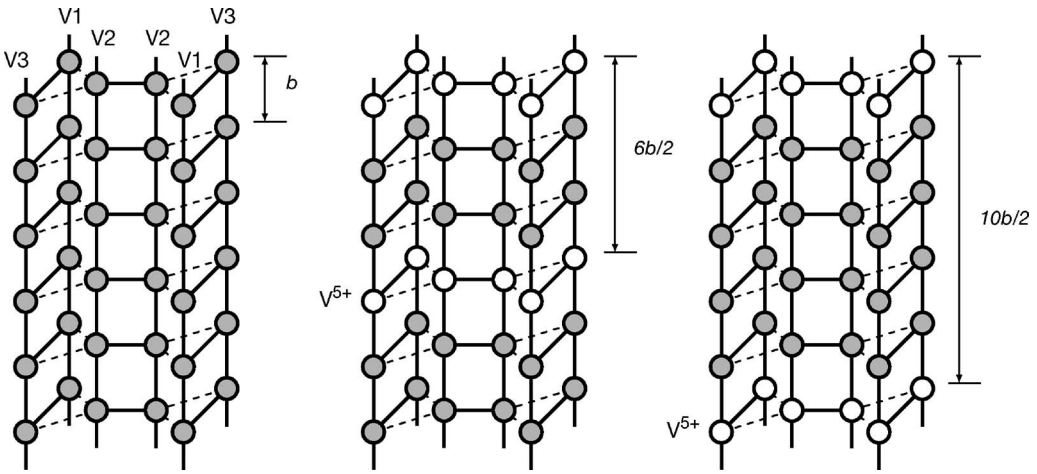

FIG. 6. Speculated charge distributions based on the coupled ladders model in charge disordered and ordered ($q=1/6b^*$ and $1/10b^*$) phases. The white and gray balls represents strict V^{5+} and intermediate $V^{4+\sim 5+}$ ions, respectively.

except $q=1/2b^*$. We cannot rule out a possibility of $1/2b^*$ superstructure caused from CO, because the $1/2b^*$ superstructure from Sr ordering which penetrates from CO to CDO phases would mask $q=1/2b^*$ spots from CO.

Very recent neutron diffraction and NMR studies on isostructural β-$Na_{0.33}V_2O_5$ reveal remarkable features in its CO phase.[8,15,16] These studies claim that the valence states of vanadium atoms show a disproportionation into strict 5+ state ($3d^0$) and intermediate states between 5+ and 4+ ($3d^\delta$: $\delta<1$) in its CO phase. Furthermore, V^{5+} ions order in a manner with the threefold periodicity along the *b* axis to form "walls" perpendicular to the *b* axis at ambient pressure. As mentioned above, the sixfold periodicity is attributed to the two fold by *A*-cation order multiplied by the threefold by CO.[4,16,8] Based on the picture in β-$Na_{0.33}V_2O_5$, we will discuss the CO in β-$Sr_{0.33}V_2O_5$.

Naively, the intermediate valence states in vanadium atoms seem to be explained by charge density wave (CDW) which is well observed in quasi-one-dimensional systems. Here, note the direction and periodicity of CDW should be determined by the nesting vector of Fermi surface. It is unnatural to suppose the Fermi surface change corresponding to $1/6b^*$-$1/10b^*$-$1/2b^*$ shift without the changes of crystal structure and carrier number in the system. Thus, even though $1/6b^*$ superstructure is explained by CDW, other periodicity such as $1/10b^*$ and/or $1/2b^*$ could not be explained. This implies that these peculiar charge modulations along the *b* axis can be attributed to CO mechanism such as intersites Coulomb interactions rather than CDW mechanism.

The fact that multiple phases with different *q* vectors exist in the CO phase reminds us "devil's staircase"-type phase diagram in α'-NaV_2O_5.[17] A large number of transitions successively takes place among higher-order commensurate phases and these are well reproduced by the axial next-nearest-neighbor Ising (ANNNI) model which was discussed by Bak and von Boehm[18] to describe frustrated Ising spin systems. Since β-$Sr_{0.33}V_2O_5$ is a 1/6-filled compound ($V^{4+}/V=1/3$), differing from a quarter-filled α'-NaV_2O_5 ($V^{4+}/V=1/2$), a threefold and its multiplied-fold periodicity such as a sixfold seem to be understandable as a simple mapping model of the charges in the lattice, but the observed 10-fold periodicity cannot be simply understood in the light of the carrier concentration and crystallographic feature of β-$Sr_{0.33}V_2O_5$. Therefore the $q=1/10b^*$ suggests a possible "devil's staircase"-type phase diagram and charge frustration mechanism.

However, the *P-T* phase diagram itself does not exactly correspond to that of ANNNI model.[18] It should be noted that β-$Sr_{0.33}V_2O_5$ has *no* distinct charge contrast which can be mapped into Ising spin model as discussed in α'-NaV_2O_5. Furthermore, the change of periodicity of the charge modulation which are described as an order structure of V^{5+} ($3d^0$) "walls" perpendicular to the *b*-axis requires the change of carrier number between two neighbor V^{5+} "walls," in contrast to the constant charge numbers within stacking layers in α'-NaV_2O_5. This situation should make the system complex. Thus, further theoretical and experimental investigations are required to explain the *P-T* phase diagram of β-$Sr_{0.33}V_2O_5$. We are now planning synchrotron radiation experiments to determine the phase diagram more precisely and to explore various modulation structures predicted by "devil's staircase"-type phase transition.

Finally, we discuss the magnetic features of β-$Sr_{0.33}V_2O_5$. All $1/6b^*$, $1/10b^*$, and $1/2b^*$ phases show spin-gap behaviors, in contrast, gapless antiferromagnetic ordering behaviors were observed in the $1/6b^*$ CO phases of A^+ compounds (A=Li, Na, Ag). Here we base on the recent Hückel tight-binding calculation on β-$Sr_{0.33}V_2O_5$ (Ref. 5) which revealed that the electronic structure can be considered as weakly coupled two kinds of two-leg ladders; V1-V3 and V2-V2 as mentioned above (see Fig. 1).

Referring to the charge distribution of CO phase in β-$Na_{0.33}V_2O_5$,[8,16] it should be likely that these coupled ladders are cut by V^{5+} ($3d^0$) "walls" arranged in the periodic manners along the *b* axis, resulting in "blocks" partitioned by two neighbor V^{5+} "walls" (see Fig. 6). Thus the carriers (electrons) are presumably confined in these "blocks" as an isolated spin system which is illustrated schematically as connected several gray balls (intermediate valence vanadium

atoms) in Fig. 6. Note that even numbers of electrons are always confined in each "block" in A^{2+} compound for every periodicity. The number of electrons in the "block" necessarily depend on the periodicity $1/(2nb^{*})$ $(n=3,5,1)$, and it is nominally estimated at $2n$ $(n=3,5)$ and 4 $(n=1)$. These electrons are distributed onto $6(n-1)$ vanadium atoms in the "block" in this coupled ladder model. On the other hand, three (odd number) electrons are confined in each "block" for the $1/6b$ structure of A^{+} compound. We can naturally suppose that even numbers of electron have a tendency toward spin-gap nature as observed in β-$Sr_{0.33}V_2O_5$, while an odd number (3) of electron is fair to spin-gapless nature (AF ordering) as in β-$Na_{0.33}V_2O_5$.

Furthermore, this spin-gap "block" seems favorable to explain Q independent (nondispersive) aspects of spin excitation which were observed in inelastic neutron excitation measurements at ambient pressure.[11]

The authors thank K. Ohwada, H. Nakao, S. Nagai, and M. Itoh for fruitful discussions. The authors also thank H. Takagi, for an experimental facility on high pressure resistivity measurements.

*Electronic address: yamauchi@issp.u-tokyo.ac.jp

[1] T. Schneider and J. M. Singer, *Phase Transition Approach to High Temperature Superconductivity* (Imperial College Press, London, 1994); E. Dagotto, T. Hotta, and A. Moreo, Phys. Rep. **344**, 1 (2001).

[2] T. Yamauchi, Y. Ueda, and N. Môri, Phys. Rev. Lett. **89**, 057002 (2002).

[3] T. Yamauchi, M. Isobe, and Y. Ueda, Solid State Sci. **7**, 874 (2005).

[4] J. I. Yamaura, M. Isobe, H. Yamada, T. Yamauchi, and Y. Ueda, J. Phys. Chem. Solids **63**, 957 (2002).

[5] M.-L. Doublet and M.-B. Lepetit, Phys. Rev. B **71**, 075119 (2005).

[6] J. Kikuchi (private communication). The ^{51}V NMR spectra down to 5 K on powder sample of β-$Pb_{0.33}V_2O_5$ do not show any splitting behavior with decreasing temperature as observed in other β-vanadium bronzes.

[7] T. Yamauchi, M. Isobe, and Y. Ueda, J. Magn. Magn. Mater. **272**, 442 (2004).

[8] S. Nagai, M. Nishi, K. Kakurai, Y. Oohara, H. Yoshizawa, H. Kimura, Y. Noda, B. Grenier, T. Yamauchi, J. I. Yamaura, M. Isobe, Y. Ueda, and K. Hirota, J. Phys. Soc. Jpn. **74**, 1297 (2005).

[9] M. Isobe and Y. Ueda, Mol. Cryst. Liq. Cryst. Sci. Technol., Sect. A **341**, 271 (2000).

[10] M. Itoh, N. Akimoto, H. Yamada, M. Isobe, and Y. Ueda, J. Phys. Soc. Jpn. **69**, Suppl. B, 155 (2000).

[11] M. Nishi (private communication). The spin dynamics in β-$Sr_{0.33}V_2O_5$ obtained by means of inelastic neutron scattering measurements using powder samples clearly shows spin gap nature and the gap energy is obtained at 6 meV and the Q dependence of the energy is almost flat. The spin gap disappeared at 33 K corresponding with the energy of 2.8 meV.

[12] T. Yamauchi and H. Ueda (unpublished).

[13] T. Yamauchi, H. Ueda, J. I. Yamaura, K. Ohwada, and Y. Ueda (unpublished).

[14] M. Suto, K. Yamashita, H. Suzuki, K. Yoshimi, S. Kimura, H. Mori, T. Kawamoto, T. Mori, Y. Nishio, and K. Kajita, J. Phys. Soc. Jpn. **74**, 2061 (2005).

[15] T. Suzuki, I. Yamauchi, M. Itoh, T. Yamauchi, and Y. Ueda, Phys. Rev. B **73**, 224421 (2006).

[16] M. Itoh, I. Yamauchi, T. Kozuka, T. Suzuki, T. Yamauchi, J. I. Yamaura, and Y. Ueda, Phys. Rev. B **74**, 054434 (2006).

[17] K. Ohwada, Y. Fujii, N. Takesue, M. Isobe, Y. Ueda, H. Nakao, Y. Wakabayashi, Y. Murakami, K. Ito, Y. Amemiya, H. Fujihisa, K. Aoki, T. Shobu, Y. Noda, and N. Ikeda, Phys. Rev. Lett. **87**, 086402 (2001).

[18] Per Bak and J. von Boehm, Phys. Rev. B **21**, 5297 (1980).